Biophys. Struct. Mech. 6, 253–270 (1980)

Biophysics of Structure and Mechanism

A New Pathway in the Photoreaction Cycle of Trans-Bacteriorhodopsin and the Absorption Spectra of its Intermediates

T. Iwasa*, F. Tokunaga*, and T. Yoshizawa

Department of Biophysics, Faculty of Science, Kyoto University, Kyoto 606, Japan

Abstract. The intermediates of trans-bacteriorhodopsin (*trans*-bR) in the photoreaction cycle were investigated under two different conditions. In a low salt and neutral pH medium (10 mM phosphate buffer, pH 6.6), *trans*-bR was irradiated with 500 nm light at −190° C, resulting in formation of *batho-trans*-bR (*batho*-bR^t). On warming in the dark, *batho*-bR^t converted to *lumi-trans*-bR (*lumi*-bR^t), *meta-trans*-bR (*meta*-bR^t) and finally to *trans*-bR. The intermediates N and O, which had been detected by others by flash photolysis, were not observed. The thermal decay of *lumi*-bR^t in a high salt and high pH medium (10 mM borate buffer with 1 M NaCl, pH 10.0) proceeded simultaneously through two pathways; one to *meta*-bR^t and another to *trans*-bR. About 72% of *lumi*-bR^t converted to *trans*-bR directly and the residue converted to *meta*-bR^t. By use of this value, the absorption spectra of *batho*-bR^t (λ_{max}: 626 nm), *lumi*-bR^t (λ_{max}: 543 nm) and *meta*-bR^t (λ_{max}: 418 nm) were calculated. A photoreaction cycle of bacteriorhodopsin was proposed on the basis of the above findings.

Key words: Low temperature spectrophotometry – Purple membrane – Bacteriorhodopsin – Photoreaction cycle – Absorption spectra of intermediates.

Introduction

Like visual pigment, bacteriorhodopsin (bR) in purple membrane of *Halobacterium halobium* is a photosensitive chromoprotein having retinal as its chromophore (Oesterhelt and Stoeckenius 1971; Blaurock and Stoeckenius 1971). On absorption of light, however, this protein plays a role in the formation of a proton gradient across the cell membrane (Oesterhelt and Stoeckenius 1973;

* *Present address:* Department of Physics, Faculty of Science, Tohoku University, Aobayama, Sendai, Japan

0340–1057/80/0006/0253/$ 3.60

Danon and Stoeckenius 1974), by which ATP is synthesized (Racker and Stoeckenius 1974; Michel and Oesterhelt 1976) and transport of cations such as Na^+ and K^+ (Lanyi et al. 1976) are regulated.

In order to elucidate these mechanisms, we started an investigation of the photoreaction of bR at liquid nitrogen temperatures a few years ago (Tokunaga et al. 1976). When light-adapted bR (bR^L; we named this compound *trans*-bR because it has all-*trans* retinal as its chromophore) (Maeda et al. 1977; Pettei et al. 1977) absorbed a photon, it converted to an intermediate named *batho-trans*-bR (this name is not meant to imply that the chromophore is in the *trans* form, but only indicates a *batho*-intermediate formed from *trans*-bR. The intermediate was designated as *batho*-bR^t). *Batho*-bR^t thermally reverted to the initial *trans*-bR (Tokunaga et al. 1976).

Flash photolysis experiments (Dencher and Wilms 1975; Chu Kung et al. 1975; Lozier et al. 1975), showed the existence of several kinds of intermediates, such as *L, M, N,* and *O* in the photoreaction cycle. However, there does not seem to be common agreement as to the existence of the intermediates. Accordingly, the thermal reactions in the photoreaction cycle of *trans*-bR should be investigated in detail.

The present report deals primarily with the thermal reactions which occur upon warming after the irradiation of *trans*-bR at low temperatures. Since the photoreaction cycle of bR is affected by solvents, pH and salt concentration (Dencher and Wilms 1975), two media were used; one was a high salt and high pH medium (10 mM borate buffer with 1 M NaCl, pH 10.0), and another was a low salt and neutral pH medium (10 mM phosphate buffer, pH 6.6).

Materials and Methods

Preparation of Purple Membrane

Purple membrane was prepared according to the method described by Oesterhelt and Stoeckenius (1974) with some modification. *Halobacterium halobium* R_1 was cultured in a medium (pH 7.0) composed of 250 g NaCl, 2.0 g KCl, 40 g Mg_2SO_4, 3.0 g sodium citrate, 5.0 g sodium maleate, 0.2 g $CaCl_2$, and 10 g bacteriological peptone (Oxoid) in 1 liter for about 4 days under vigorous aeration. After reaching a steady state of growth of the bacterial cells, air was changed to nitrogen gas. The culture was irradiated by fluorescent lamps for several days until the purple membrane attained full growth.

The cells were harvested by centrifugation at 8,000 *g* for 20 min, and then washed with a basal salt (the culture medium without bacteriological peptone) twice. DNase was added to the cell suspension in the basal salt, and then the suspension was dialysed against 10 mM phosphate buffer (pH 6.6) to puncture the cells. The lysate was centrifuged at 100,000 *g* for 30 min, and the purple membrane was precipitated. The precipitate was washed with the phosphate buffer 3 or 4 times, and then put on a linear sucrose density gradient (30–50%, W/V) with 60% sucrose as the bottom cushion. Centrifugation at 100,000 *g* for 17 h in a Hitachi RPS 25 rotor formed a band composed of only purple

membrane. The purple membrane band was collected, from which the sucrose was removed by dialysis against 10 mM phosphate buffer overnight.

The purple membrane was suspended in 10 mM phosphate buffer with glycerol at a final concentration of 75% (V/V). This suspension was used as a sample for low temperature spectrophotometry.

Spectrophotometry

Absorption spectra at low temperatures were measured with a Dewar specially constructed for the Hitachi 323 or Shimadzu MPS 5000 recording spectrophotometer (Yoshizawa 1972). On the warming experiments, as soon as the sample was warmed to a certain temperature, it was recooled to −90 or −190° C for measurement of the absorption spectrum. On cooling to −50° C, microcrystals sometimes appeared in the sample, which caused scattering of the measuring light, resulting in declination of the base line. The declination was diminished by use of an opal glass just behind an optical cell (light pass; 1 mm). The temperature of the sample was monitored with a copper-constantan thermocouple inserted in a copper block in which the sample was fixed. A 500 W Xe lamp (Ushio) was used as a light source for irradiation of the sample. The wavelength of the irradiation ligth was selected by inserting a glass cut-off and/or an interference filter (Toshiba) into the irradiation light beam.

Results

I. Purple Membrane in a Low Salt and Neutral pH Medium (10 mM Phosphate Buffer, pH 6.6)

Trans-bR in 10 mM phosphate buffer with 75% of glycerol at 0° C has its λ_{max} at 572 nm. On cooling to liquid nitrogen temperature (−190° C), λ_{max} moved to 583 nm (curve 1 in Fig. 1a). On irradiating *trans*-bR at −190° C with green light at 500 nm, the absorption spectrum displayed a bathochromic shift with an isosbestic point at 594 nm. Finally, a photosteady state (curve 2 in Fig. 1a) was formed (designated as State^{L}), which consisted of *trans*-bR and *batho*-bR^{t} (corresponding to K; Lozier et al. 1975). State^{L} and *trans*-bR are perfectly interconvertible by light, as with animal rhodopsin. These results coincided with our results reported previously (Tokunaga et al. 1976).

In order to investigate the thermal reaction of *batho*-bR^{t}, State^{L} was gradually warmed up to a required temperature in the dark, and then immediately recooled to −190° C for measurement of the absorption spectrum. Up to −120° C, the absorption spectrum scarcely changed. Above this temperature, the spectrum shifted to shorter wavelength with an isosbestic point at 570 nm (curves 3 ~ 5 in Fig. 1b). The absorbance at wavelengths longer than 570 nm decreased and increased at shorter wavelengths. This result showed that *batho*-bR^{t} was stable below −120° C and, above this temperature, it converted

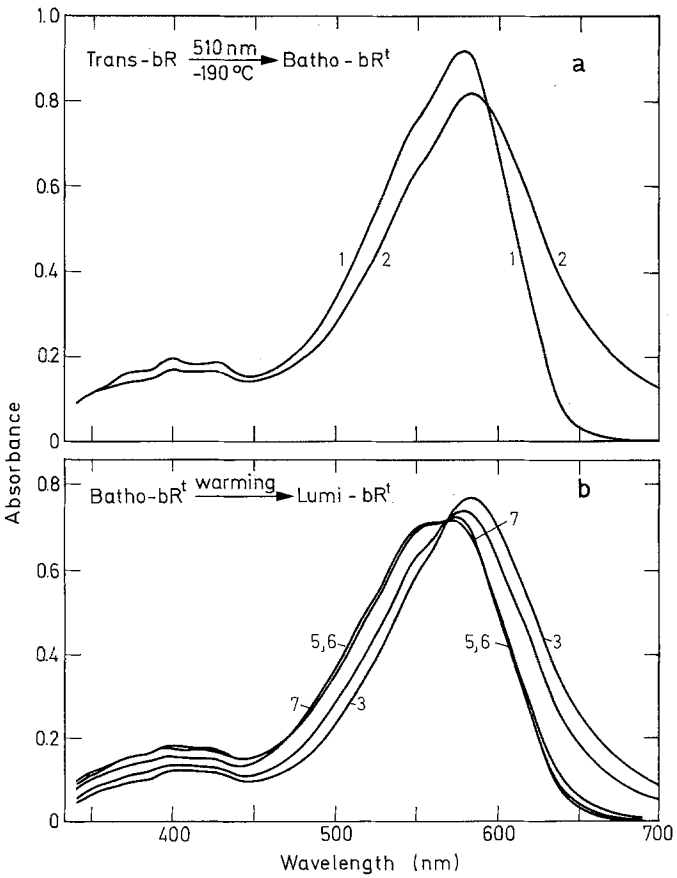

Fig. 1. The photoreaction and the thermal reaction of *trans*-bR in the low salt and neutral pH medium. **a** Curve 1: *Trans*-bR at −190° C. *Trans*-bR was formed by the irradiation of bR with 500 nm light at 0° C. Curve 2: State^L (photosteady state), which was formed by irradiating *trans*-bR with 500 nm light for 10 min at −190° C. **b** Thermal conversion of *batho*-bR^t to *lumi*-bR^t by gradual warming. All the spectra were measured at −190° C. Curve 3: The spectrum of the State^L at −190° C composed of *trans*-bR and *batho*-bR^t. Curves 4 ~ 7: Products of warming in the dark successibely to −120, −105, −95, and −90° C, respectively. Each time the preparation was recooled to −190° C for recording the spectrum. Curves 3 ~ 6 form an isosbestic point at 570 nm. Curve 7 does not pass through the isosbestic point. **c** Thermal conversion of *lumi*-bR^t by gradual warming. All the spectra were measured at −90° C. Curve 7: A mixture of *trans*-bR and *lumi*-bR^t at −90° C (identical with curve 7 in Fig. 1b). Curves 8 ~ 10: Products of warming in the dark successibely to −80, −70, and −60° C, respectively. There are four isosbestic points at 377, 450, 557, and 630 nm. **d** Thermal conversion of *meta*-bR^t to *trans*-bR by gradual warming. All the spectra were measured at −90° C. Curves 11 ~ 15: Products of warming in the dark successively to −50, −40, −30, −20, and −10° C, respectively. Curves 14 and 15 are similar to the spectrum of *trans*-bR at −90° C

to another intermediate. Since both warming to −105 and to −95° C gave the same spectrum (curves 5 and 6 in Fig. 1b), the intermediate should be stable below −95° C. The difference spectrum between curve 6 (that warmed to −95° C) and curve 3 (State^L) has a maximum at 510 nm. Since this maximum is quite similar to that between L and *trans*-bR, which had been identified by a

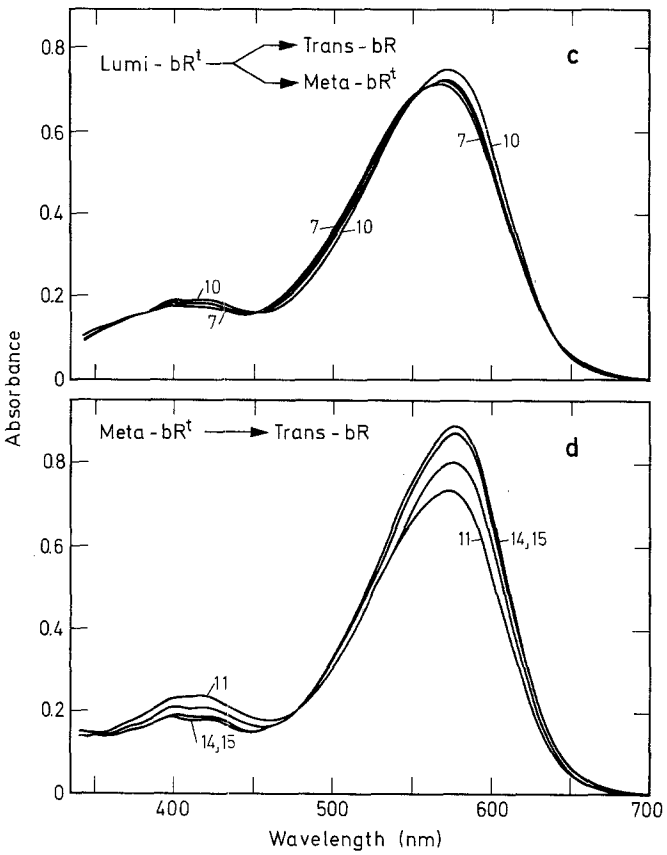

flash photolytic experiment (Lozier et al. 1975), we termed this intermediate *lumi-trans*-bR (*lumi*-bR^t). The spectrum of the sample warmed to −90° C showed a shoulder around 550 nm at −190° C (curve 7 in Fig. 1b), while the spectrum at −90° C did not show it (Fig. 1c). The appearance of the shoulder may be due to sharpening of the absorption band due to cooling.

The thermal reaction of *lumi*-bR^t was investigated by warming, and recooling immediately to −90° C for measurement of the absorption spectrum. Up to −60° C, the absorption spectrum changed gradually with four isosbestic points at 377, 450, 557, and 630 nm (Fig. 1c). The absorbances between 450 and 557 nm, at wavelengths shorter than 377 nm and at wavelengths longer than 630 nm decreased and those at the other wavelengths increased.

Above −50° C, the absorption spectrum behaved differently, that is, the absorbances in a wavelength region shorter than 463 nm decreased, and those in a wavelength region longer than 463 nm increased (Fig. 1d). The absorption spectrum of the sample warmed above −20° C (curves 14 and 15) coincided with that of *trans*-bR. Thus, *trans*-bR displayed a cyclic photoreaction.

In Figure 1d, an isosbestic point lies at 463 nm, which is the same as that between *M* and *trans*-bR, and also the difference spectrum between curve 11 and

curve 15 is similar to that between *M* and *trans*-bR (Lozier et al. 1975; Becher and Ebrey 1977). Thus, the spectral change shown in Figure 1d should be the thermal back reaction of *meta-trans*-bR (we named *M meta-trans*-bR, which was designated as *meta*-bR^t) to *trans*-bR.

The spectral changes shown in Figure 1c, which form four isosbestic points, are not so simple, and one cannot explain them as only due to the decay of *lumi*-bR^t to *meta*-bR^t. It is probable that the decrease of absorbances between 450 and 557 nm, and the increase between 377 and 450 nm, are due to decay of *lumi*-bR^t and formation of *meta*-bR^t, respectively. In addition, the increase of absorbance in a wavelength region longer than 557 nm indicates a formation of a molecular species other than *meta*-bR^t, because *meta*-bR^t has no absorbance at wavelengths longer than 480 nm (see Fig. 6; Oesterhelt and Hess 1973).

Is the molecular species a new product? Since Figure 1d shows only the conversion of *meta*-bR^t to *trans*-bR, and the final curve (curve 15) is the same as the original *trans*-bR, we assume the molecular species is *trans*-bR.

A question arises as to whether or not this *trans*-bR is a direct product of *lumi*-bR^t. This question can be formulated in two possible schemes:

Scheme 1: *lumi*-bR^t → *meta*-bR^t → *trans*-bR

Lumi-bR^t fully converts to *meta*-bR^t, but the conversion of *meta*-bR^t to *trans*-bR is so rapid that one can observe only a small increase of the absorbance due to *meta*-bR^t. The increase in the wavelength region longer than 557 nm is then due to *trans*-bR formed from *meta*-bR^t.

Scheme 2: *lumi*-bR^t → *meta*-bR^t
lumi-bR^t → *trans*-bR

Lumi-bR^t converts directly to both *meta*-bR^t and *trans*-bR. The increase of absorbance in the longer wavelength region is then due to *trans*-bR directly formed from *lumi*-bR^t.

In order to examine which scheme is correct, some experiments described in the next section were performed at conditions where *meta*-bR^t is stable.

II. Purple Membrane in a High Salt and High pH Medium (10 mM Borate Buffer with 1 M NaCl, pH 10.0)

It has been reported that *meta*-bR^t is relatively stable in ether or in a high salt and high pH medium (Oesterhelt and Hess 1973; Becher and Ebrey 1977). Using the high salt and high pH medium, we examined the thermostability of *meta*-bR^t.

Purple membrane in the high salt and high pH medium and 75% glycerol was irradiated at −50° C with light at wavelengths longer than 560 nm. All the *trans*-bR in the preparation converted to *meta*-bR^t with a clear isosbestic point at 463 nm (Fig. 2a). *Meta*-bR^t at −50° C has λ_{max} at 418 nm and two shoulders

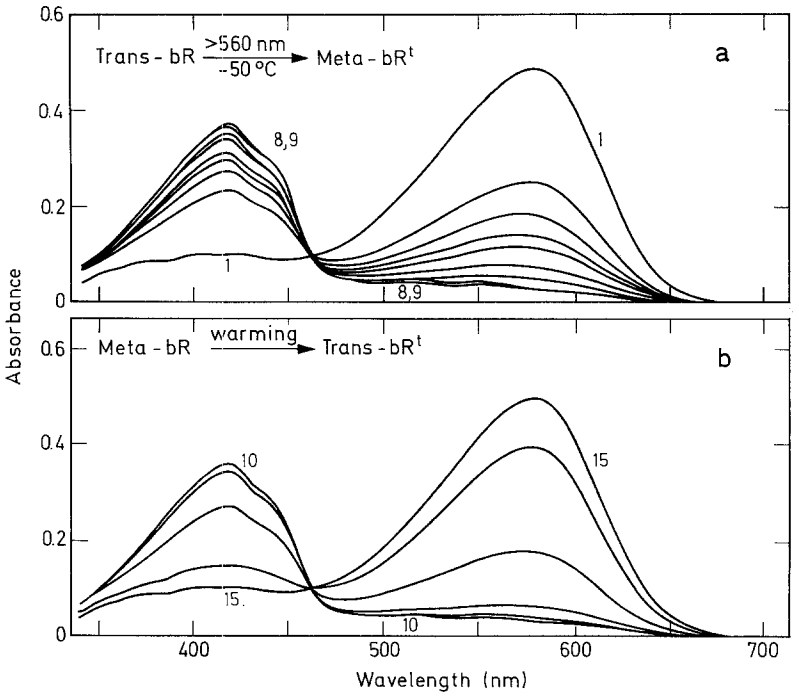

Fig. 2. Photoconversion of *trans*-bR to *meta*-bR^t and its thermal reversion in the high salt and high pH medium. **a** The course of photoconversion of *trans*-bR to *meta*-bR^t. Curve 1: *Trans*-bR. Curves 2 ~ 9: Products of successive irradiation with light at wavelengths longer than 560 nm at −50° C for 1, 1, 2, 4, 8, 16, 32, and 64 min. All the *trans*-bR converted to *meta*-bR^t. The residual absorbance in the longer wavelength region is presumably due to some contaminated carotenoid. **b** The course of reversion of *meta*-bR^t to *trans*-bR by gradual warming. Curve 10: Redrawn from curve 9 in Fig. 2a. Curves 11 ~ 15: Products formed by warming in the dark to −40, −30, −20, −10, and 0° C, respectively. Curve 15 represents *trans*-bR. All the spectra were measured at −50° C

around 395 and 440 nm. The residual absorbance in the longer wavelength region is probably due to a little contamination of a carotenoid (bacterioruberin) (curve 9 in Fig. 2a). The spectrum of *meta*-bR^t did not change within 30 min in the dark at −50° C. Upon warming above −30° C in the dark, *meta*-bR^t converted back to *trans*-bR (curves 10 ~ 15 in Fig. 2b) with a clear isosbestic point at 463 nm, which lies at the same wavelength as that found in the photoreaction of *trans*-bR to *meta*-bR^t. It is certain that *meta*-bR^t is stable at −50° C in the high salt and high pH medium.

Now the question whether Scheme 1 or 2 is correct can be examined by warming *lumi*-bR^t in the high salt and high pH medium to −50° C, under the assumption that the photoreaction cycle of bR in this medium is not different from that in low salt and neutral pH medium. Some increase of the absorbance in the wavelength region longer than 557 nm, as shown in Figure 1c (formation of *trans*-bR), will support Scheme 2 and some decrease in the same region (formation of *meta*-bR^t) will support Scheme 1.

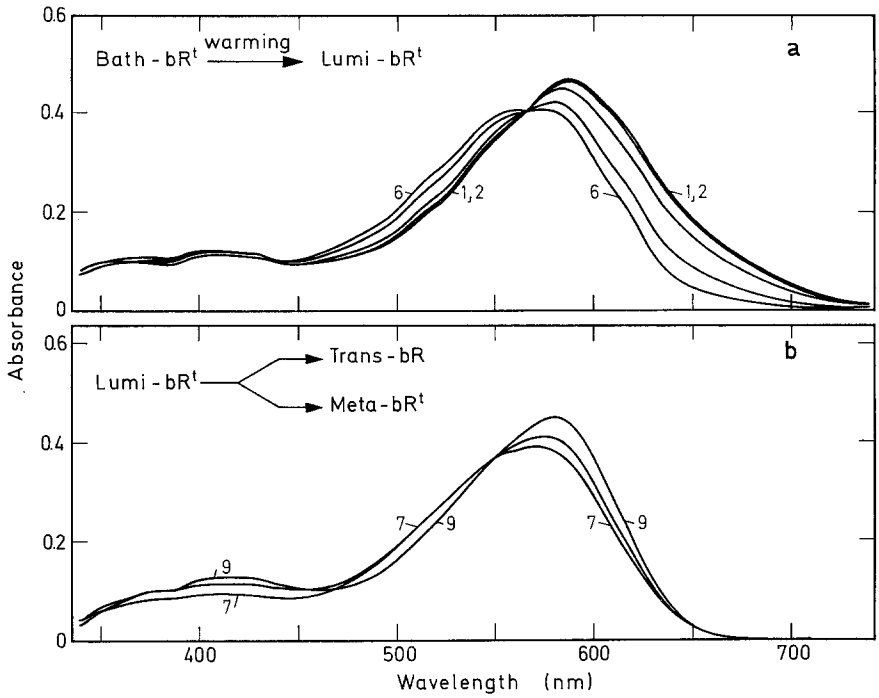

Fig. 3. The thermal reaction of *batho*-bR^t in a high salt and high pH medium. **a** The course of thermal conversion of *batho*-bR^t to *lumi*-bR^t. All the spectra were measured at −190° C. Curve 1: State^L produced by irradiating *trans*-bR at −190° C with 500 nm light. Curves 2 ~ 6: Products formed by warming in the dark to −150, −130, −110, −100, and −90° C, respectively. **b** The thermal conversion of *lumi*-bR^t. All the spectra were measured at −90° C. Curve 7: Redrawn from curve 6 in Figure 3a. Curves 8 and 9: Products formed by warming to −70 and −50° C, respectively

Thus, our experiment began with checking the thermal stability of *meta*-bR^t at −50° C. The sample containing *meta*-bR^t was warmed to 0° C in the dark in order to change all the *meta*-bR^t to *trans*-bR. After cooling the sample to −190° C, it was irradiated with 500 nm light. *Trans*-bR converted to *batho*-bR^t in the same manner as that in the low salt and neutral pH medium. Then the *batho*-bR^t was warmed in the same manner as in Sect. I. In the high salt and high pH medium, *batho*-bR^t converted to *lumi*-bR^t with somewhat anbiguous curve-intersection points (Fig. 3a), though in the low salt and neutral pH medium this spectral change (curve 3 ~ 6 in Fig. 1b) showed a sharp isosbestic point at 570 nm. It is not clear yet why the curve-intersection point moves towards shorter wavelengths in the high salt and high pH medium. Anyway, all the *batho*-bR^t converted to *lumi*-bR^t at −90° C.

Then, *lumi*-bR^t was gradually warmed to −70° or −50° C, and immediately recooled to −90° C. The absorbance around 510 nm decreased and those around 410 and 580 nm increased (Fig. 3b). These spectral changes support Scheme 2 as already mentioned. Thus *trans*-bR can be formed directly from *lumi*-bR^t.

III. Calculation of the Absorption Spectra of Batho-bR^t and lumi-bR^t

Since we have found conversions of *lumi*-bR^t to both *trans*-bR and *meta*-bR^t, curves 7 and 9 in Figure 3b can be formulated as follows:

$$A^{\text{curve 7}} = C^R\varepsilon^R + C^L\varepsilon^L \tag{1}$$

$$A^{\text{curve 9}} = C^R\varepsilon^R + \alpha C^L\varepsilon^M + \beta C^L\varepsilon^R \tag{2}$$

$$\alpha + \beta = 1 \tag{3}$$

C^R and C^L are the concentrations of *trans*-bR and *lumi*-bR^t, respectively. ε^R, ε^L, and ε^M are the molar extinction coefficients of *trans*-bR, *lumi*-bR^t, and *meta*-bR^t, respectively. The initial concentration of *trans*-bR, designated as C, is equal to the sum of the concentrations of *trans*-bR and *lumi*-bR^t.

$$C = C^R + C^L. \tag{4}$$

If the value of C^L/C (the fraction of *lumi*-bR^t contained in curve 7 in Fig. 3b) is known, the absorption spectrum of *lumi*-bR^t can be estimated. However, one cannot get C^L/C directly, so that we began with the calculation of the fraction of *lumi*-bR^t converted to *meta*-bR^t, ($\alpha C^L/C$), followed by obtaining equations for the calculation of β (or α) and C^L/C, estimating the difference spectrum between *lumi*- and *meta*-bR^t, and finally calculating their absorption spectra.

i) Estimation of C^L/C. The difference absorbance between curves 7 and 9 ($A^{\text{curve 7–9}}$) can be expressed as follows:

$$\begin{aligned} A^{\text{curve 7–9}} &= \alpha C^L(\varepsilon^L - \varepsilon^M) + \beta C^L(\varepsilon^L - \varepsilon^R) \qquad (5^*) \\ &= \alpha C^L(\varepsilon^L - \varepsilon^R) - \alpha C^L(\varepsilon^M - \varepsilon^R) + \beta C^L(\varepsilon^L - \varepsilon^R) \\ &= C^L(\varepsilon^L - \varepsilon^R) - \alpha C^L(\varepsilon^M - \varepsilon^R). \qquad (5) \end{aligned}$$

As seen in Figure 4b (curve 2), the difference spectrum between *lumi*-bR^t and *trans*-bR, (A^{L-R}), intersects with the abscissa at 525 nm, where ε^R equals to ε^L. Thus,

$$A_{525}^{\text{curve 7–9}} = -\alpha C^L(\varepsilon_{525}^M - \varepsilon_{525}^R) \tag{6}$$

$\alpha C^L/C$ can be calculated from $A_{525}^{\text{curve 7–9}}$ (Fig. 4a) and $C(\varepsilon_{525}^M - \varepsilon_{525}^R) = A_{525}^{M-R}$ (curve 1 in Fig. 4b) as follows:

$$\frac{-\alpha C^L}{C} = \frac{A_{525}^{\text{curve 7–9}}}{A_{525}^{M-R}} = \frac{0.078 \times 0.3}{0.47 \times (-0.53)} = -0.0939$$

$$\alpha = 0.094 \times \frac{C}{C^L} \tag{7}$$

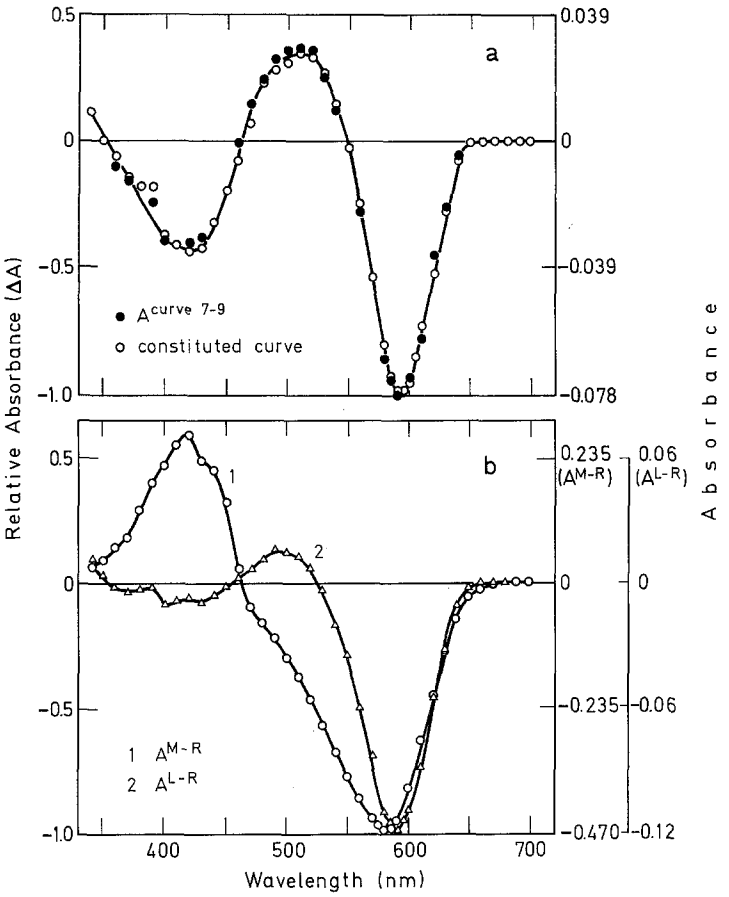

Fig. 4. a The spectral change of thermal decay of *lumi*-bR^t in the high salt and high pH medium. − ● −: The difference spectrum between curves 7 and 9 ($A^{\text{curve } 7-9}$) in Figure 3b. This curve is normalized at its difference maximum (595 nm) as 1.0. The absolute difference absorbance (right ordinate) at 595 nm is 0.078. − ○ −: Difference spectrum constituted from the difference spectrum between *meta*-bR^t and *trans*-bR (A^{M-R}; curve 1 in Fig. 4b), and that between *trans*-bR and *lumi*-bR^t (A^{L-R}; curve 2 in Fig. 4b). **b** The difference spectra used for constitution of the difference spectrum shown in Figure 4a. Curve 1: A^{M-R} at −90° C. Spectra of *meta*-bR^t (curve 10 in Fig. 2b) and *trans*-bR (curve 15 in Fig. 2b) were measured at −90° C and then difference spectrum between them were calculated. Curve 2: A^{L-R} at −90° C, estimated from curve 7 in Figure 3b and curve 15 in Figure 2b measured at −90° C. These difference spectra are normalized at their difference minima as −1.0 at 580 and 590 nm, respectively. The original difference absorbances (right ordinate) at the minima are 0.47 and 0.12, respectively

Inserting α into Eq. (5),

$$A^{\text{curve } 7-9} = C^L(\varepsilon^L - \varepsilon^R) - 0.094\, C(\varepsilon^M - \varepsilon^R)\,. \tag{8}$$

Now, $A^{\text{curve } 7-9}$ can be constituted from $C^L(\varepsilon^L - \varepsilon^R)$ (curve 2 in Fig. 4b) and $C(\varepsilon^M - \varepsilon^R)$ (curve 1 in Fig. 4b). The constituted curve (− ○ − in Fig. 4a) is almost identical to $A^{\text{curve } 7-9}$ (− ● −). This is a reaffirmation of the conclusion that *lumi*-bR^t converted to both *trans*-bR and *meta*-bR^t.

ii) Equations for Estimation of β and C^L/C. In Eq. (5*), $A^{\text{curve } 7-9}$ are shown in Fig. 4a and $C^L(\varepsilon^L-\varepsilon^R)$ corresponds to curve 2 in Figure 4b. $\alpha C^L(\varepsilon^L-\varepsilon^M)$ can be replaced by 0,094 $C(\varepsilon^L-\varepsilon^M)$ from Eq. (7). Thus, β, which is the fraction of *lumi*-bR^t converted to *trans*-bR, can be expressed by the following equation,

$$\beta = \frac{A^{\text{curve } 7-9} - 0.094\ C(\varepsilon^L - \varepsilon^M)}{C^L(\varepsilon^L - \varepsilon^R)}. \tag{9}$$

Since $\alpha = 1-\beta$, α can be estimated. Using Eq. (7), one can get the value of C^L/C, which is the fraction of *lumi*-bR^t contained in curve 7 in Figure 3b. Thus, the absorption spectra of intermediates can be estimated, if the difference spectrum between *lumi*-bR^t and *meta*-bR^t is estimated, though it cannot be obtained by the warming experiments (Fig. 1c, 1d, and 3b).

iii) Difference Spectrum Between lumi- and meta-bR^t. *Trans*-bR was irradiated for 10 min at various temperatures with light at wavelengths longer than 560 nm. At $-70°$ C, the absorbance in a wavelength region shorter than 510 nm increased with a small peak at about 410 nm, due to the formation of *meta*-bR^t (curve 2 in Fig. 5a). The absorbance at the peak increased with a rise in temperature (curves $3 \sim 5$ in Fig. 5a). The temperature dependence of the spectral change is shown clearly in the insert in Figure 5a, where the absorbance changes at 410 nm and at 510 nm after 10 min irradiation at various temperatures are plotted. The absorbance at 410 nm, mainly due to *meta*-bR^t, increased with a rise in temperature up to $-50°$ C, while the absorbance at 510 nm, due to *lumi*-bR^t (see Fig. 6), decreased. These changes indicate that the amount of *meta*-bR^t produced by the irradiation increased up to $-50°$ C, and also no or little formation of *lumi*-bR^t occurred at $-40°$ C.

Now, one can estimate the difference spectrum between *meta*-bR^t and *lumi*-bR^t using the results shown in Figure 5a. The photoreactions in Figure 5a can be expressed as follows:

$$C\ \textit{trans}\text{-bR} \xrightarrow{h\nu} C_T^R\ \textit{trans}\text{-bR} + C_T^L\ \textit{lumi}\text{-bR}^t + C_T^M\ \textit{meta}\text{-bR}^t$$

$$C = C_T^R + C_T^L + C_T^M,$$

where C is a molar concentration of the original *trans*-bR, and C_T^R, C_T^L and C_T^M are concentration of *trans*-bR, *lumi*-bR^t and *meta*-bR^t at $T°$ C, respectively. Thus, the difference spectra in Figure 5b can be expressed as follows:

$$(C_T^L\varepsilon^L + C_T^M\varepsilon^M) - (C - C_T^R)\varepsilon^R. \tag{10}$$

Assuming that C_{-40}^L and C_{-70}^M are very low (see the insert in Fig. 5a), curves 2-1 and 5-1 in Figure 5b can be expressed by $aC_{-70}^L(\varepsilon^L-\varepsilon^R)$ and bC_{-40}^M $(\varepsilon^M-\varepsilon^R)$, which were normalized at their minima as -1.0 with normalizing factors a and b, respectively. Thus, the secondary difference absorbance (Δ^2A) between curves 5-1 and 2-1 (curve 1 in Fig. 5c, $-\,\bigcirc\,-$) was expressed as follows:

$$\Delta^2A = bC_{-40}^M\,\varepsilon^M - aC_{-70}^L\,\varepsilon^L + (aC_{-70}^L - bC_{-40}^M)\,\varepsilon^R. \tag{11}$$

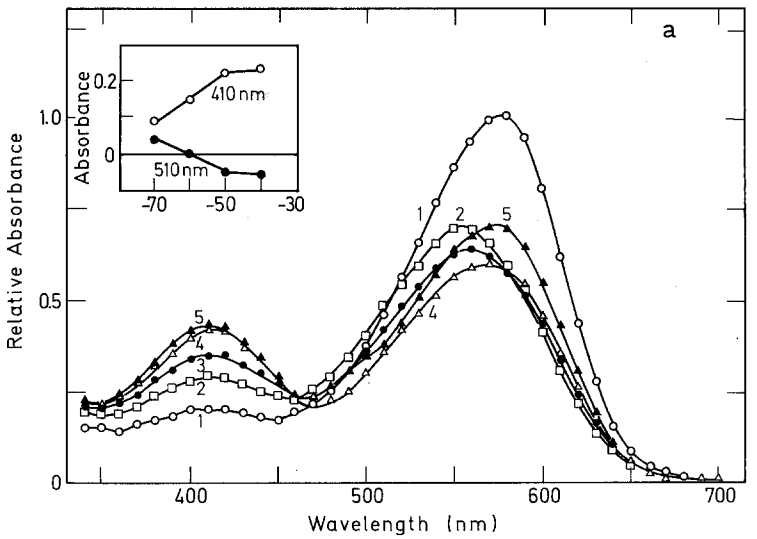

Fig. 5. Estimation of the difference spectrum between *lumi*-bR^t and *meta*-bR^t. **a** Spectral change of *trans*-bR irradiated at different temperatures with orange light at wavelengths longer than 560 nm for 10 min. Curve 1: *Trans*-bR in low salt and neutral pH medium at −70° C. Curves 2 ~ 5: Products of irradiation at −70, −60, −50, and −40° C, respectively. *Inserted:* The changes of absorbances at 410 nm (− ○ −) and 510 nm (− ● −), where the λ_{max} of *meta*-bR^t and the difference maximum between *lumi*-bR^t and *trans*-bR lie, respectively, are plotted against the temperatures at which the sample was irradiated. **b** Difference spectra before and after the irradiation of *trans*-bR at different temperatures. Curves 2-1 ~ 5-1: The difference spectra between curve 1 and curves 2, 3, 4, or 5 in Figure 5a, respectively. Those difference spectra were normalized at their difference minima as −1.0. **c** Calculation of the difference spectrum between *lumi*-bR^t and *meta*-bR^t. Curve 1 (− ○ −): The difference spectrum between curves 5-1 and 2-1 in Figure 5b. Curve 2 (− × −): The difference spectrum between *meta*-bR^t and *trans*-bR, which was redrawn from curve 5-1 in Figure 5b for calculation of curve 3. The absorbance was adjusted to zero for the wavelength region longer than 630 nm when it was added to curve 1. Curve 3 (− □ −): The calculated difference spectrum between equi-molar *meta*-bR^t and *lumi*-bR^t

Curve 1 in Figure 5c has two peaks (at 410 nm and at 610 nm) and one trough (at 535 nm), which are due to $bC^M_{-40}\varepsilon^M$, $(aC^L_{-70}-bC^M_{-40})\varepsilon^R$ and $aC^L_{-70}\varepsilon^L$, respectively.

In order to remove the absorbance change due to $(aC^L_{-70}-bC^M_{-40})\varepsilon^R$, $(aC^L_{-70}-bC^M_{-40})$ $(\varepsilon^M-\varepsilon^R)$ was added to Δ^2A so as to make the absorbances at wavelengths longer than 630 nm of curve 1 in Figure 5c zero. This shown by the following equations:

$$\begin{aligned}\Delta^2A + (aC^L_{-70} - bC^M_{-40})(\varepsilon^M - \varepsilon^R) \\ = bC^M_{-40}\,\varepsilon^M - aC^L_{-70}\,\varepsilon^L + aC^L_{-70}\,\varepsilon^M - bC^M_{-40}\,\varepsilon^M \\ = aC^L_{-70}\,(\varepsilon^M - \varepsilon^L)\,. \qquad (12)\end{aligned}$$

The spectrum $(aC^L_{-70}-bC^M_{-40})$ $(\varepsilon^M-\varepsilon^R)$ added is shown as curve 2 in Figure 5c. Thus, the difference spectrum between *lumi*-bR^t and *meta*-bR^t (curve 3 in

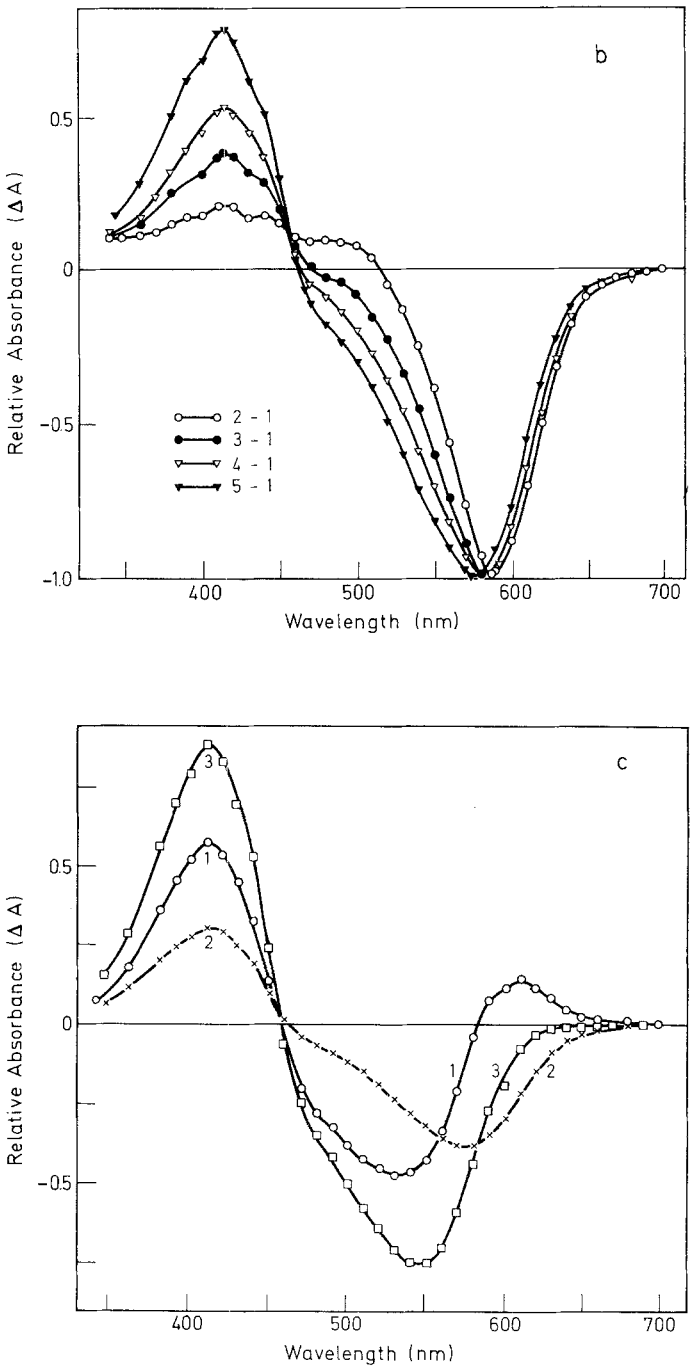
b
0.5
0
-0.5
-1.0
Relative Absorbance (Δ A)
2 - 1
3 - 1
4 - 1
5 - 1
400
500
600
700
Wavelength (nm)
c
3
1
2
0.5
0
-0.5
Relative Absorbance (Δ A)
1
3
2
400
500
600
700
Wavelength (nm)

Fig. 5.

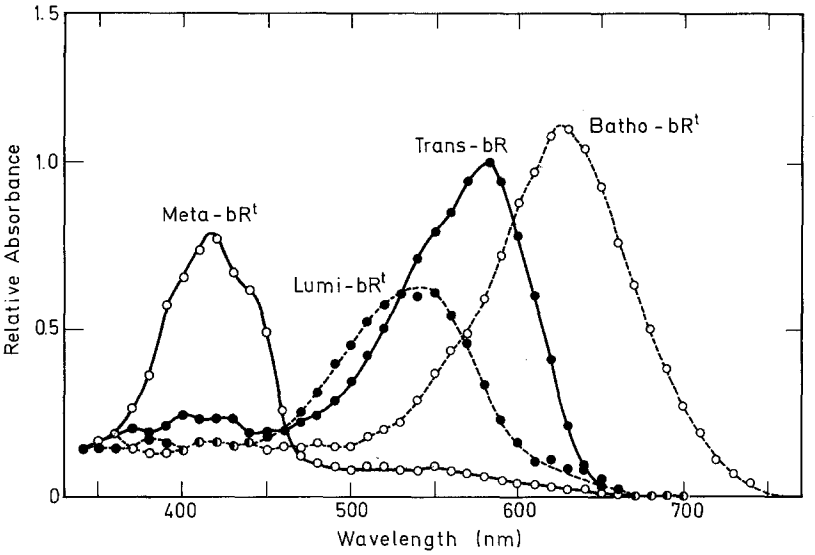

Fig. 6. The absorption spectra of *trans*-bR and its intermediates. – ● –: *Trans*-bR (λ_{max}: 583 nm, −190° C). – – ○ – –: *Batho*-bR^t (λ_{max}: 626 nm, −190° C). – – ● – –: *Lumi*-bR^t (λ_{max}: 543 nm, −90° C). – ○ –: *Meta*-bR^t (λ_{max}: 418 nm, −90° C). The spectrum of each intermediate is normalized to maximal absorbance of *trans*-bR at the same temperature

Fig. 5c) was estimated assuming that the difference spectrum, which was estimated from the spectra obtained under the low salt and neutral pH conditions, is not different in shape from that at the high salt and high pH conditions.

iv) Absorption Spectra. For the calculation of the absorption spectra of intermediates, the value of aC^L_{-70} in Eq. (12) or aC^L_{-70}/C was required. We estimated aC^L_{-70}/C using the difference spectrum between *meta*-bR^t and *trans*-bR, $C(\varepsilon^M-\varepsilon^R)$ (curve 1 in Fig. 4b). The difference spectra $C(\varepsilon^M-\varepsilon^L)$ and $C(\varepsilon^M-\varepsilon^R)$ cross each other at 525 nm, because $C(\varepsilon^M-\varepsilon^L)-C(\varepsilon^M-\varepsilon^R) = C(\varepsilon^R-\varepsilon^L)$ equals to zero at 525 nm as shown in Figure 4b. aC^L_{-70} $(\varepsilon^L-\varepsilon^M)$ (curve 3 in Fig. 5c) was multiplied by a certain factor (0.365) to cross at 525 nm with $C(\varepsilon^M-\varepsilon^R)$. Thus, $C(\varepsilon^M-\varepsilon^L)$ was determined.

Using Eq. (9), one can calculate the value of β. We got 0.723 as an average for β at 10 wavelengths between 540 and 650 nm, indicating that 72.3% of *lumi*-bR^t converted to *trans*-bR directly. α was also obtained from the equation $\alpha + \beta = 1$. C^L/C was calculated as 0.339 from Eq. (7). This value means that curve 7 in Figure 3b was composed of 33.9% of *lumi*-bR^t and 66.1% of *trans*-bR. This also indicates that 33.9% of the initial pigment caused the photoreaction and converted to *batho*-bR^t, if *batho*-bR^t converts into *lumi*-bR^t without any other reactions.

The absorption spectra of *lumi*-bR^t (at −90° C) and *batho*-bR^t (at −190° C) were estimated by subtracting 66% of *trans*-bR from curve 7 in Figure 3b and

curve 1 in Figure 3a, respectively. These spectra are shown in Figure 6 with those of *trans*-bR (at −190° C) and *meta*-bR^t (at −90° C).

Finally, the thermal reaction of *batho*-bR^t (Fig. 3a and 3b) can be understood as follows: Irradiation of *trans*-bR at liquid nitrogen temperatures formed a photosteady state composing 66.1% of *trans*-bR and 33.9% of *batho*-bR^t (curve 1 in Fig. 3a). *Batho*-bR^t converted to *lumi*-bR^t thermally. *Lumi*-bR^t had two reaction pathways, that is, 72.3% of *lumi*-bR^t converted to *trans*-bR directly and the rest (27.7%), corresponding to nearly 10% of the initial pigments, converted to *meta*-bR^t.

Discussion

By means of low temperature spectrophotometry, we confirmed the presence of three intermediates (*batho*-bR^t, *lumi*-bR^t, and *meta*-bR^t) in the reaction cycle of *trans*-bR, but we could not observe any other intermediates in the process of *meta*-bR^t to *trans*-bR, corresponding to intermediate *N* or *O*, which had been detected by flash photolysis (Dencher and Wilms 1975; Lozier et al. 1975). There are two possible reasons why the intermediates *N* and *O* were not detected by low temperature spectrophotometry. One is that the rate of the *meta*-bR^t to *N* reaction may be slower than that of *N* to *O*. Under such conditions, the life time of *N* becomes very short and it converts to the next intermediate very rapidly. If the life time of *N* is very short (within a few seconds even at low temperatures), it is impossible to detect such an intermediate with a conventional spectrophotometer. The same may be true in the case of *O*. In animal rhodopsin system, however, the rates of the thermal reactions of the intermediates are slow enough to detect them with flash photolysis and low temperature spectrophotometry (Cone 1972).

Another reason is that the thermal reaction of *meta*-bR^t may have at least two reaction pathways in the thermal decay. This means that *N* and *O* may be by-products. Sherman et al. (1976b) observed that in the presence of valinomycin or Na^+ in the purple membrane preparation, the formation of *O* (660 nm species) was inhibited together with some increase of the life time of the 410 nm transient (*meta*-bR^t). Furthermore, the rate constant and activation energy for the decay of *meta*-bR^t are different from those for the formation of *O* (660 nm species) in the temperature range 0 ~ 60° C (Sherman et al. 1976a), suggesting that these two intermediates occupied parallel pathways. Korenstein et al. (1978) also suggested a branching pathway for the thermal reaction in the photocycle of *trans*-bR. Their reason for the suggested existence of two conformations of *meta*-bR^t was based on the observations that the decay of *meta*-bR^t was composed of two exponentials. However, we have no evidence to support the existence of two conformations, because the back reaction of *meta*-bR^t to *trans*-bR at several temperatures below 0° C fitted a single exponential curve (not shown). The discrepancy between Korenstein et al. (1978) and us may be explained by an assumption that *meta*-bR^t converts mainly to *trans*-bR below 0° C, but at higher temperatures it converts to *N* and *O*. This assumption is consistent with an observation by Sherman et al. (1976a).

Table 1. Absorption maximum (λ_{max}) and molar extinction coefficient (ε) of intermediates in the photocycle of *trans*-bR. The molar extinction coefficients were calculated according to that of *trans*-bR as 63,000. The number in ( ) represents the temperature

	Present work		Becher et al.		Chu Kung et al.		Lozier et al.	
	λ_{max} (nm)	$\varepsilon \times 10^3$	λ_{max} (nm)	$\varepsilon \times 10^3$	λ_{max} (nm)	$\varepsilon \times 10^3$	λ_{max} (nm)	$\varepsilon \times 10^3$
Trans-bR	583 (−190)	63	568 (23)	63	563 (−25)	63	570 (1)	63
Batho-bR^t	626 (−190)	69	628 (−196)	86	631 (−25)	78	590 (1)	53
Lumi-bR$_t$	543 (−90)	40	547 (−100)	51	520 (−25)	51	550 (1)	46
Meta-bR^t	418 (−90)	49	412 (−40)	45	418 (−25)	70	412 (1)	41
	Low temperature spectrophotometry				Flash photolysis			

We showed that the reaction pathway of *trans*-bR was branched at *lumi*-bR^t, and only 28% of *lumi*-bR^t converted to *meta*-bR^t below −50° C. However, whether or not *lumi*-bR^t converts at room temperature to both *meta*-bR^t and *trans*-bR with the same ratio as measured at low temperatures remaines unsettled. The ratio seems to depend on the $\Delta G^{\neq}$ of the reaction of *lumi*-bR^t to *meta*-bR^t or *trans*-bR.

The absorption spectra of the intermediates have been reported by several groups (Table 1). Assuming that all the *batho*-bR^t converts to *meta*-bR^t, Becher et al. (1978) calculated the molar extinction coefficient of *batho*-bR^t to be about 86,000, which is larger than our value, 69,000. It is certain that their assumption led to some increase in the molar extinction coefficient of *batho*-bR^t, because the ratio of the intermediate to *trans*-bR in the preparation had been estimated as less than the true ratio. Lozier and Niederberger (1977) also calculated the absorption spectrum of *batho*-bR^t, assuming that the quantum efficiency of *trans*-bR is independent of wavelength. If the quantum efficiency of *trans*-bR is independent of wavelength, one can calculate the absorption spectrum of *batho*-bR^t from absorption spectra of photosteady state mixtures (Fisher 1967). According to Hurley and Ebrey (1978), the position of the isosbestic point in the conversion of *trans*-bR to *batho*-bR^t depends on the wavelengths of the irradiation light of *trans*-bR. In such a case, the calculation according to Fisher (1967) does not give the correct absorption spectrum. They showed that the λ_{max} of *batho*-bR^t lies at 590 nm, which is at a shorter wavelength than found by others.

We have investigated the photoreaction of *trans*-bR under low salt and neutral pH conditions, and under high salt and high pH conditions. No difference was found in shape of the absorption spectrum of *trans*-bR or its product formed by warming of State^L (compare Fig. 1b and 1c with Fig. 3a and

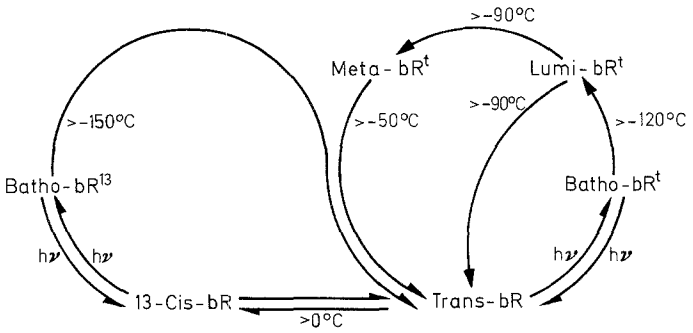

Fig. 7. Photoreaction cycle of bacteriorhodopsin. Photochemical reactions are designated by *hv* and thermal (dark) reactions, by the transient temperatures of intermediates to their products

3b, respectively) between the two media. Thus, our assumption for the calculation of the absorption spectra did not result in a significant difference from the real spectra. The high salt and high pH medium stabilized only *meta*-bR^t. *Batho*-bR^t and *lumi*-bR^t decayed to the next intermediates at about -120 and $-90°$ C in both media, respectively.

On the basis of the present results and the investigation of the photoreaction cycle of 13-*cis*-bR, a synthetic pigment from 13-*cis* retinal and bacteriopsin, the photoreaction cycle of bacteriorhodopsin was drawn as shown in Figure 7. Bacteriorhodopsin at physiological temperatures has two different states; one is the light-adapted state (bR^L) and another is the dark-adapted state (bR^D). The chromophore of bR^D is an equi-molar mixture of 13-*cis* and all-*trans* retinals (Maeda et al. 1977; Pettei et al. 1977). We have already reported that bR having 13-*cis* retinal as its chromophore (bR$_1$ in Tokunaga et al. 1976) has a *batho*-intermediate different from that of *trans*-bR (Tokunaga et al. 1976). Thus, the photoreaction cycle of bacteriorhodopsin is composed of 13-*cis*-bR and *trans*-bR cycles; 13-*cis*-bR has no *lumi*- and *meta*-intermediates, but only *batho*-intermediate (*batho*-13-*cis*-bR; designated as *batho*-bR^{13}). Details of the photoreaction cycle of 13-*cis*-bR will be published elsewhere.

Acknowledgement. This work was supported in part by the grant from Japanese Ministry of Education to T. Y.

References

Becher B, Ebrey T (1977) The quantum efficiency for the photochemical conversion of the purple membrane protein. Biophys J 17: 185–191

Becher B, Tokunaga F, Ebrey TG (1978) Ultraviolet and visible absorption spectra of the purple membrane protein and the photocycle intermediates. Biochemistry 17: 2293–2300

Blaurock AE, Stoeckenius W (1971) Structure of the purple membrane. Nature [New Biol] 233: 152–155

Chu Kung M, Devault D, Hess B, Oesterhelt D (1975) Photolysis of bacterial rhodopsin. Biophys J 15: 907–911

Cone RA (1972) Rotational diffusion of rhodopsin in the visual receptor membrane. Nature [New Biol] 236: 39–43

Danon A, Stoeckenius W (1974) Photophosphorylation in *Halobacterium halobium*. Proc Natl Acad Sci USA 70: 2853–2857

Dencher N, Wilms M (1975) Flash photometric experiments on the photochemical cycle of bacteriorhodopsin. Biophys Struct Mech 1: 259–271

Fisher E (1967) The calculation of photostationary states in system A $\rightleftarrows$ B when only A is known. J Phys Chem 71: 3704–3706

Hurley JB, Ebrey TG (1978) Energy transfer in the purple membrane of *Halobacterium halobium*. Biophys J 22: 49–66

Korenstein R, Hess B, Kushimitz D (1978) Branching reactions in photocycle of bacteriorhodopsin. FEBS Lett 93: 266–270

Lanyi JK, Renthal R, MacDonald RE (1976) Light induced glutamate transport in *Halobacterium halobium* envelope vesicles. II: Evidence that the driving force is a light-dependent sodium gradient. Biochemistry 15: 1603–1609

Lozier RH, Bogomolni RA, Stoeckenius W (1975) Bacteriorhodopsin: A light-driven proton pump in *Halobacterium halobium*. Biophys J 15: 955–962

Lozier RH, Niederberger W (1977) The photochemical cycle of bacteriorhodopsin. Fed Proc 36: 1805–1809

Maeda A, Iwasa T, Yoshizawa T (1977) Isomeric composition of retinal chromophore in dark-adapted bacteriorhodopsin. J Biochem (Tokyo) 82: 1599–1604

Michel H, Oesterhelt D (1976) Light induced change of the pH-gradient and the membrane potential in *Halobacterium halobium*. FEBS Lett 65: 175–178

Oesterhelt D, Hess B (1973) Reversible photolysis of the purple complex in the purple membrane of *Halobacterium halobium*. Eur J Biochem 37: 316–326

Oesterhelt D, Stoeckenius W (1971) Rhodopsin-like protein from the purple membrane of *Halobacterium halobium*. Nature [New Biol] 233: 149–152

Oesterhelt D, Stoeckenius W (1973) Functions of a new photoreceptor membrane. Proc Natl Acad Sci USA 70: 2853–2857

Oesterhelt D, Stoeckenius W (1974) Isolation of the cell membrane of *Halobacterium halobium* and its fractionation into red and purple membrane. In: Fleisher S, Packer L (eds) Methods in enzymology, Vol 31: Biomembranes Part A. Academic Press, New York, pp 667–678

Pettei MJ, Yudd AP, Nakanishi K, Henselman R, Stoeckenius W (1977) Identification of retinal isomers isolated from bacteriorhodopsin. Biochemistry 16: 1955–1959

Racker E, Stoeckenius W (1974) Reconstitution of purple membrane vesicles catalyzing light-driven proton up-take and adenosine triphosphate formation. J Biol Chem 249: 662–663

Sherman WV, Korenstein R, Caplan SR (1976a) Energetics and chronology of phototransients in the light response of the purple membrane of *Halobacterium halobium*. Biochim Biophys Acta 430: 454–458

Sherman WV, Silfkin NA, Caplan SR (1976b) Kinetic studies of phototransients in bacteriorhodopsin. Biochim Biophys Acta 423: 238–248

Tokunaga F, Iwasa T, Yoshizawa T (1976) Photochemical reaction of bacteriorhodopsin. FEBS Lett 72: 33–38

Yoshizawa T (1972) The behaviour of visual pigments at low temperatures. In: Dartnall HJA (ed) Handbook of sensory physiology, Vol VII/1: Photochemistry of vision. Springer, Berlin Heidelberg New York, pp 146–179

Received 28 November 1979/Accepted 7 May 1980